Original Article

MOLECULAR METABOLISM

The brown adipose tissue glucagon receptor is functional but not essential for control of energy homeostasis in mice

Jacqueline L. Beaudry [1], Kiran Deep Kaur [1], Elodie M. Varin [1], Laurie L. Baggio [1], Xiemin Cao [1], Erin E. Mulvihill [1,4], Jennifer H. Stern [2,6], Jonathan E. Campbell [1,5], Phillip E. Scherer [2], Daniel J. Drucker [1,3,*]

ABSTRACT

Objective: Administration of glucagon (GCG) or GCG-containing co-agonists reduces body weight and increases energy expenditure. These actions appear to be transduced by multiple direct and indirect GCG receptor (GCGR)-dependent mechanisms. Although the canonical GCGR is expressed in brown adipose tissue (BAT) the importance of BAT GCGR activity for the physiological control of body weight, or the response to GCG agonism, has not been defined.

Methods: We studied the mechanisms linking GCG action to acute increases in oxygen consumption using wildtype (WT), *Ucp1*$^{-/-}$ and *Fgf21*$^{-/-}$ mice. The importance of basal GCGR expression within the *Myf5*$^{+}$ domain for control of body weight, adiposity, glucose and lipid metabolism, food intake, and energy expenditure was examined in *Gcgr*$^{BAT-/-}$ mice housed at room temperature or 4 °C, fed a regular chow diet (RCD) or after a prolonged exposure to high fat diet (HFD).

Results: Acute GCG administration induced lipolysis and increased the expression of thermogenic genes in BAT cells, whereas knockdown of *Gcgr* reduced expression of genes related to thermogenesis. GCG increased energy expenditure (measured by oxygen consumption) both *in vivo* in WT mice and *ex vivo* in BAT and liver explants. GCG also increased acute energy expenditure in *Ucp1*$^{-/-}$ mice, but these actions were partially blunted in *Ffg21*$^{-/-}$ mice. However, acute GCG administration also robustly increased oxygen consumption in *Gcgr*$^{BAT-/-}$ mice. Moreover, body weight, glycemia, lipid metabolism, body temperature, food intake, activity, energy expenditure and adipose tissue gene expression profiles were normal in *Gcgr*$^{BAT-/-}$ mice, either on RCD or HFD, whether studied at room temperature, or chronically housed at 4 °C.

Conclusions: Exogenous GCG increases oxygen consumption in mice, also evident both in liver and BAT explants *ex vivo*, through UCP1-independent, FGF21-dependent pathways. Nevertheless, GCGR signaling within BAT is not physiologically essential for control of body weight, whole body energy expenditure, glucose homeostasis, or the adaptive metabolic response to cold or prolonged exposure to an energy dense diet.

Keywords Glucagon; brown adipose tissue; Energy expenditure; Adiposity; Lipolysis; Thermogenesis

1. INTRODUCTION

The proglucagon-derived peptides (PGDPs) are encoded by a single mammalian gene and include glucagon (GCG), oxyntomodulin, glicentin, and two GCG-like peptides, GLP-1 and GLP-2 [1]. The PGDPs control energy intake, gut motility, mucosal integrity, and the absorption, disposal and storage of ingested energy. The prototype member of the PGDP family, 29 amino acid GCG, is produced in and secreted from islet α-cells, and to a lesser extent, from brainstem neurons [1]. The principal biological role of pancreatic GCG is the maintenance of euglycemia through its control of hepatic glucose production [2–4].

GCG exerts its metabolic actions through a single GCG receptor (GCGR) [5] highly expressed in hepatocytes but also detected in brain, heart, kidney, gastrointestinal tract, and both white and brown adipose tissue (WAT and BAT, respectively) [6,7]. Although less extensively studied, GCG exerts direct actions on adipose tissue, encompassing increased blood flow, stimulation of lipolysis, increased glucose uptake and

[1]Lunenfeld-Tanenbaum Research Institute, Mt. Sinai Hospital, Toronto, Ontario, Canada [2]Touchstone Diabetes Center, Department of Internal Medicine, The University of Texas Southwestern Medical Center, Dallas, USA [3]Department of Medicine, University of Toronto, Toronto, Ontario, Canada

[4] Current address: University of Ottawa Heart Institute, 40 Ruskin Street, Ottawa, ON H-3228A, Canada.
[5] Current address: Duke Molecular Physiology Institute, 49–102, 300 N. Duke St. Durham, NC 27701, USA.
[6] Current address: University of Arizona, College of Medicine, Division of Endocrinology, 1501 N. Campbell Ave. Tucson, AZ 85724-5035.

*Corresponding author. E-mail: drucker@lunenfeld.ca (D.J. Drucker).

Abbreviations: GCG, Glucagon; GCGR, Glucagon receptor; iBAT, interscapular brown adipose tissue; eWAT, epididymal white adipose tissue; iWAT, inguinal white adipose tissue; rWAT, retroperitoneal white adipose tissue; mWAT, mesenteric white adipose tissue; Tb, body temperature; UCP1, uncoupling protein 1; FGF21, Fibroblast growth factor 21; TGs, Triglycerides; NEFAs, non-esterified fatty acids; RER, Respiratory exchange ratio; β-3-adrenergic receptor agonist, CL316,243

Received January 14, 2019 • Revision received January 28, 2019 • Accepted January 29, 2019 • Available online xxx

https://doi.org/10.1016/j.molmet.2019.01.011

increased oxygen consumption in WAT and BAT [8–12]. In addition, GCG administration also acutely increases whole body oxygen consumption following administration to animals and humans *in vivo* [13–15].

Considerable evidence links sustained GCG administration to the reduction of food intake, enhancement of energy expenditure and weight loss in rodent and human studies [16–18]. Moreover, patients presenting with GCG-producing tumors frequently manifest severe weight loss, through mechanisms that are incompletely understood [19]. Despite several decades of experimentation, the precise processes and cell types contributing to GCG-mediated weight loss remain incompletely understood. Although intracerebroventricular infusion of GCG directly reduces food intake [20] and increases energy expenditure [21], other studies have demonstrated that the GCG-mediated reduction of food intake requires intact hepatic vagal nerve innervation [22] and rats with surgical BAT denervation exhibit diminished metabolic and mitochondrial responses to exogenous glucagon [23].

The clinical development of investigational GCG-containing multi-agonists, including oxyntomodulin and its derivatives [3,24,25], for the treatment of diabetes and obesity has rekindled interest in whether and how GCGR signaling results in BAT activation and increased energy expenditure [2,26,27]. Several studies invoke an indirect role for GCG on BAT and energy expenditure, acting through enhanced blood flow [28], the sympathetic nervous system (SNS) [29,30], or fibroblast growth factor (FGF)21 [31,32]. However, other studies support a direct role for GCG as an activator of oxygen consumption in BAT [14,33]. Interestingly, GCG infusion in healthy humans subjected to cold exposure increased energy expenditure without evidence for BAT activation as assessed by positron emission tomography scanning [15].

Here we examined the importance of the BAT GCGR for GCG-stimulated energy expenditure in mice and characterized the metabolic phenotype of mice with genetic deletion of the *Gcgr* in BAT using myogenic factor 5 (*Myf5*)-Cre. Using BAT cells and explants *ex vivo*, as well as WT and knockout mice, we demonstrate that GCG acts both directly and indirectly to enhance whole body and BAT oxygen consumption. Nevertheless, the BAT *Gcgr* is physiologically dispensable for GCG-stimulated increase in energy expenditure, and the adaptive metabolic responses to HFD feeding or prolonged cold exposure.

2. MATERIALS AND METHODS

2.1. Animals

All animal experiments were conducted in accordance with protocols approved by the Toronto Centre for Phenogenomics (TCP) Animal Care Committee. Experiments were performed in group-housed male mice that were maintained on a 12h light/dark cycle at room temperature (RT; 21 °C), 4 °C, or 30 °C and with free access to food and water, except where indicated. Mice were fed either a standard rodent chow diet (RCD; 18% kcal from fat, 2018 Harlan Teklad, Mississauga, ON) or a high-fat diet (HFD; 45% kcal from fat, D12451i, Research Diets, New Brunswick, NJ) for diet-induced obesity analysis. Chronically housed (~12 weeks) 4 °C group-housed male mice were placed into non-vented microisolator cages (Ancare) with free access to food and water and transferred into environmentally controlled enclosures (Betatech Inc.) at 8–10 weeks of age with an ambient temperature of initially 16 °C. The ambient temperatures within the enclosures were decreased by 2 °C every day until 4 °C ambient temperature was established.

$Gcgr^{BAT-/-}$ (BAT-specific *Gcgr* knockout) mice and controls (Cre, Floxed) were generated by crossing hemizygous *Myf5*-Cre mice (007893, The Jackson Laboratory, Bar Harbour, ME) with floxed *Gcgr* mice [34,35]. Experiments were carried out in all groups of male mice (unless otherwise stated) that were on a C57BL/6J background. However, because the control groups were phenotypically similar with respect to body weight, fat mass, and glucose homeostasis, all control data are presented as a single pooled group (*Myf5*-Cre and $Gcgr^{flox/flox}$ mice). Mice were euthanized by CO_2 inhalation, and tissues were immediately frozen in liquid nitrogen or placed in tissue cassettes for histology analysis. Whole-body $Ucp1^{-/-}$ (003124) mice were purchased from The Jackson laboratory. Whole-body $Fgf21^{-/-}$ ($Fgf^{21tm1.1Djm}$) mice were provided by Steven A. Kliewer [36].

2.2. Body composition using MRI (magnetic resonance imaging), food intake, indirect calorimetry and *ex vivo* respirometry

Body composition was measured after 32 weeks on RCD or HFD using an Echo MRI nuclear magnetic resonance system (Echo Medical Systems, Houston, TX). Food intake was quantified (over 72 hrs) at 8–10 and 30–32 weeks of age in mice housed individually in cages containing pre-weighed amounts of food. Food intake data in this paper are shown from mice maintained on diet for 30–32 weeks. After 16–18 weeks on RCD or HFD, mice were subjected to indirect calorimetry experiments to measure oxygen consumption, carbon dioxide production, respiratory exchange ratio, activity, and energy expenditure (kcal/h) using a Comprehensive Lab Animal Monitoring System (CLAMS; Columbus Instruments, Columbus OH). For measuring GCG-induced oxygen consumption measurements, mice were fasted for ~4 h, anesthetized with sodium pentobarbital (60 mg/kg), and placed on a heating pad for 10 mins prior to transferring them into a CLAMS chamber where they were acclimatized for ~ 8 mins and subsequently given ip injections of vehicle control (acidified PBS) followed by GCG (0.01, 0.1, or 0.5 mg/kg, Sigma, Oakville, ON) or vehicle control followed by GCG (0.5 mg/kg, Sigma), and CL316,243 (1.0 mg kg, Sigma), a selective β-3-adrenergic receptor agonist. For basal *ex vivo* oxygen consumption measurements, fresh tissues were extracted from mice after CO_2 asphyxiation and immediately placed into warm (37 °C) DMEM (4.5 g/l glucose, L-glutamine, Wisent, St. Bruno, QC) buffer. Tissues were weighed (~10–20 mg), washed in filtered respiration buffer (PBS, 0.02% fatty acid free BSA, 25 μM glucose, 0.01% (vol/vol) of 100 mM Na pyruvate (Sigma)), minced with scissors, re-suspended in respiration buffer and placed into a Mitocell chamber (MT200A, Strathkelvin Instruments, North Lanarkshire, Scotland) with a Clark electrode (Strathkelvin). For each tissue, measurements were obtained from three separate depots of equivalent size. Recordings were normalized to tissue weight. For stimulated *ex vivo* oxygen consumption measurements, tissues were extracted from littermate mice ~20–30 minutes after an acute injection of either PBS or GCG (0.5 mg/kg, Sigma).

2.3. Glucose, insulin and lipid tolerance tests

All metabolic tests were performed after a 4–5 h fast. Blood was collected via the tail vein for measuring insulin, GLP-1, GIP, GCG, triglycerides, and FGF21 at indicated time points. For oral and intraperitoneal glucose tolerance tests (oGTT and ipGTT, respectively), D-Glucose (1.5 g/kg; Sigma, Oakville, ON) was administered by oral gavage (oGTT) or ip injection (ipGTT). During insulin tolerance tests (ITT), animals fed a RCD received a single ip injection of 0.7 U/kg BW insulin (Humalog, VL7510, Eli Lily, Scarborough, ON), whereas animals fed a HFD received 1.0 U/kg BW of insulin. When mice were housed at 4 °C, all animals were given a single ip injection of 0.35 U/kg BW of insulin. Blood glucose was measured from the tail vein using a handheld glucose monitor (Contour, Bayer, Mississauga, ON)) before and

MOLECULAR METABOLISM

15, 30, 45, 60, 90, and 120 min post-glucose gavage or insulin injection. For lipid tolerance tests (LTT), animals received a 200 μl oral gavage of olive oil (Sigma) at time 0 and blood samples were collected before and 1, 2, and 3 h after gavage.

2.4. Blood collection

All blood samples (~50–100 μl) during metabolic tests were collected from tail vein into lithium coated Microvette tubes (Sarstedt, Numbrecht, Germany) and mixed with a 10% volume of TED (5000 kIU/ml Trasylol (Bayer), 32 mM EDTA, and 0.01 mM Diprotin A (Sigma)). Samples were kept on ice and plasma was collected by centrifugation (>12, 000 rpm at 4 °C for 5 minutes) and stored at - 80 °C.

2.5. Hormone and enzymatic assays

Plasma insulin (Ultrasensitive Mouse Insulin ELISA, Cat# 80-INSMSU-E01 Alpco Diagnostics, Salem, NH), total GLP-1 (Meso Scale Diagnostics, Cat# K150JVC-2 Rockville, MD), GIP (Crystal Chem, Cat# 81517, Elk Grove Village, IL), and GCG (Mercodia, Cat#10-1281-01) levels were assessed in plasma samples collected before (time 0) and 10 mins post glucose or insulin administration during metabolic tests. Plasma was assayed for non-esterified fatty acids (NEFAs) using the NEFA-HR (2) kit (Wako Diagnostics, Cat# 999-34691, 995-34791, 991-34891, 993-35191, 276-76491, Mountain View, CA) or triglycerides (TGs) using the Trig-GB kit (Cat# 05171407, calibrator 11877771216, Roche, Mississauga, ON). For determination of TGs in tissue, frozen iBAT samples were weighed (10–20 mg) and TGs were extracted using a 2:1 chloroform-methanol solution and quantified with Trig-GB kit (Roche). Plasma FGF21 (Millipore, Cat# EZRMFGF21-26K, Billerica, MA) levels were assayed in fasted (4 h) 8 week old mice fed a RCD.

2.6. RNA isolation and gene expression assays

Tissue samples were homogenized in Tri Reagent (Molecular Research Center, Cincinnati, ON) using a TissueLyser II system (Qiagen, Germantown, MD), and total RNA was extracted using the manufacturer's protocol. First strand cDNA was synthesized from DNase I-treated total RNA using the SuperScript III and random hexamers (Thermo Fisher Scientific, Markham, ON). Gene expression levels were quantified by real-time PCR using a QuantStudio System and TaqMan Gene Expression Master Mix and Assays (Thermo Fisher Scientific). Primer/probes were purchased from Thermo Fisher Scientific and are listed in Supplementary Table 1. qPCR data were analyzed by $2^{-\Delta\Delta Ct}$ method, and expression levels for each gene were normalized to either *Actb* (β-actin) or *Tbp* (TATA-box-binding protein).

2.7. Detection of full-length mouse *Gcgr* mRNA transcripts

Full-length (~1.4 kb) mouse *Gcgr* PCR products were amplified from cDNA using the following primers: forward 5′-CTG CTG CTG CTG CTG TTGG -3′ and reverse 5′-ACC TTG GGA GAC TAC TGGC-3′, separated on an agarose gel, transferred to a nylon membrane, and hybridized overnight with an internal ^{32}P-labeled mouse *Gcgr*-specific oligonucleotide probe (5′-AAT GCC ACC ACA ACC TAA GC-3'-). The membrane was washed and then imaged using a Storm 860 Phosphor Screen and Quantity One imaging software (Bio-Rad, Hercules, CA). *Actb* was used as a control for RNA integrity of samples.

2.8. Cell culture: BAT cell line

Immortalized BAT cells were a gift from Dr. Bruce Spiegelman's laboratory (Department of Cancer Biology, Dana-Farber Cancer Institute, Boston, MA) [37]. On Day 0, BAT preadipocyte cells were plated onto collagen coated plates (<0.006%) containing growth media (DMEM (4.5 g/l glucose, L-glutamine, Wisent, St. Bruno, QC) with 20% FBS (Wisent), 1% Sodium Pyruvate (100 mM, Sigma), <0.01% HEPES (1M, Wisent), and 1% Penicillin-Strep (Wisent)) and grown until they achieved a healthy mono-layer (~90–95% confluent). After reaching confluence, on Day 1, growth media was replaced with induction media (DMEM with 10% FBS, 1% Sodium Pyruvate, HEPES and 1% Penicillin-Strep supplemented with 2 μg/ml dexamethasone (Sigma), 0.5 mM 3-isobutyl-1-methylxanthine (IBMX; Sigma), 125 μM indomethacin (Sigma), 10 μg/ml or 1.7 μM insulin (Sigma), and 1 nM T3 (Sigma). After 48 h of induction, on Day 3, media was changed to maintenance media (DMEM (25 mM glucose) with 10% FBS, 1% Sodium Pyruvate, <0.01% HEPES, and 1% Penicillin-Strep supplemented with 10 μg/ml or 1.7 μM insulin and 1 nM T3, (Sigma), until cells were fully differentiated by Day 7. Fresh media was added to cells as required. All experiments, unless otherwise stated, were performed on fully differentiated cells on Day 7.

To assess the effects of GCG on gene expression or lipolysis, BAT cells were differentiated for 7 days in collagen coated 12-well cell culture dishes (initiated at a density of 40,000 cells per well) in 1 ml of growth media. On Day 7, cells were nutrient-media starved for 3 h in FBS-free DMEM media devoid of all supplements except sodium pyruvate and HEPES. For gene expression assay, BAT cells in each well were treated with media (1 ml) containing either acidified PBS or GCG 100 nM for 1 or 4 h and RNA was isolated by adding 1 ml of Tri-reagent directly into plates and homogenizing cells by repetitive pipetting. For analysis of lipolysis, BAT cells were serum starved for 3 h. Media was then changed to warm (37 °C) filtered Kreb's buffer (12 mM Hepes, 121 mM NaCl, 4.9 mM KCL, 1.2 mM MgSO4, 0.33 mM CaCl2, 3% BSA, 3 mM glucose) containing either acidified PBS or GCG (10 nM- 1 μM) for 2 h. Media was then collected into 1.5 ml Eppendorf tubes and frozen at −20 °C. Free glycerol in cell media was measured using a free glycerol assay kit (Cat# F6428, Sigma), and normalized to protein content (measured using Bradford assay kit (Bio-Rad, Montreal, QC).

2.9. siRNA-induced knockdown of *Gcgr* mRNA in BAT cells

On Day 0, BAT cells were plated at a density of 80,000 cells per well in 6-well tissue culture dishes containing growth media. Cells were differentiated as described above until Day 4, when differentiated BAT cells were trypsinized, centrifuged and re-suspended in antibiotic-free maintenance media. Differentiated BAT cells were transfected with siRNA duplexes (Universal scrambled negative control (Origene, Rockville, MD) sequence, Cat# SR30004-CGUUAAUCGCGUAUAAUACGCGUAT) or *Gcgr* (Origene duplex sequence, Cat# SR415672A-GGAGAAGCCAUGUUAUCUAUGAACT)) diluted in OptiMEM to a final concentration of 50 mM in 1 ml of media using Lipofectamine RNAiMAX Reagent (Thermo Fisher Scientific), following the manufacturer's protocol. Transfection complexes were added to collagen coated 12-well plates containing 800,000–1,000,000 cells per well suspended in antibiotic-free maintenance media. Maintenance media was replaced every 24 h until Day 7 when cells were harvested for RNA isolation as described above.

2.10. Histological analysis

Adipose tissues were fixed in 10% buffered formalin for a minimum of 48 h, and then tissues were transferred into 70% ethanol until processing. Samples were paraffin-embedded, sectioned at 4 μm thickness, slide-mounted, and stained with hematoxylin and eosin. Sections were scanned using the ScanScope CS System (Aperio

Original Article

Tehcnologies, Sausalito, CA) and digital images captured at 100 μM using ScanScope Software (Aperio Technologies).

2.11. Statistics

Data are represented as the mean ± SEM. Statistical significance was determined by one-way ANOVA (post-hoc test Bonferroni), two-way ANOVA (post-hoc test Tukey), paired (Figure 2D and Figure S2C) or unpaired two-tailed Student's t-test using GraphPad Prism version 8 Software (San Diego, CA). A p value < 0.05 was considered statistically significant.

3. RESULTS

3.1. *Gcgr* mRNA transcripts are expressed at low levels in BAT and GCG directly increases thermogenic gene expression and lipolysis in a BAT cell line

Gcgr mRNA transcripts were detected by quantitative real time PCR in adipose tissue depots (Figure 1A) including mesenteric white adipose tissue (mWAT), inguinal (iWAT), epididymal (eWAT), retroperitoneal (rWAT), and interscapular brown adipose tissue (iBAT) (Figure 1A), corresponding to full length *Gcgr* mRNA (Figure 1B), albeit at levels 1,000—10,000 fold lower than in liver (Figure 1A). *Gcgr* mRNA was also detected in a differentiated BAT cell line (Figure S1A), associated with induction of *Ucp1* expression (Figure S1B). GCG treatment increased levels of *Ucp1*, *Ppargc1a,* and *Cepba* mRNA in BAT cells studied at Day 2 of differentiation (Figure S1C) and *Ucp1*, *Ppargc1a, Cidea, Elovl3, Ptgs2*, and *Fgf21* mRNA transcripts were increased by GCG on Day 7 (Figure 1C). Conversely, siRNA-mediated knockdown of *Gcgr* expression reduced levels of *Ucp1*, *Ppargc1a, Elovl3*, *Cebpa, Cidea*, *Lipe, Ardb3*, and *Fgf21* mRNA transcripts after 2 or 7 days of differentiation (Figure 1D and Figure S1D). CL316,243 was administered to BAT cells in a separate experiment, demonstrating selective induction of mRNA transcripts in response to adrenergic activation (Figure S1E). GCG also directly increased lipolysis in a dose-dependent manner in BAT cells (Figure 1E), through mechanisms requiring the *Gcgr* (Figure S1F). Hence, BAT cells express a functional canonical GCGR directly coupled to thermogenic gene expression and lipolysis.

3.2. GCG increases oxygen consumption through UCP1-independent, FGF21-dependent pathways

Considerable evidence demonstrates that acute GCG administration rapidly increases circulating levels of FGF21 in mice and humans [31,38]. Indeed, acute GCG administration increased oxygen consumption in mice through mechanisms requiring hepatic farnesoid X receptor signaling and FGF21 [32]. We observed that GCG (0.01—0.5 mg/kg) administration rapidly increased oxygen consumption in a dose-dependent manner in RCD-fed WT mice housed at RT (Figure 2A and Figure S2A-B) and in mice fed a HFD (Figure S2C). GCG also increased oxygen consumption in WT mice acclimatized to either cold (4 °C, Figure 2B) or thermoneutral (30 °C, Figure 2C) temperatures for

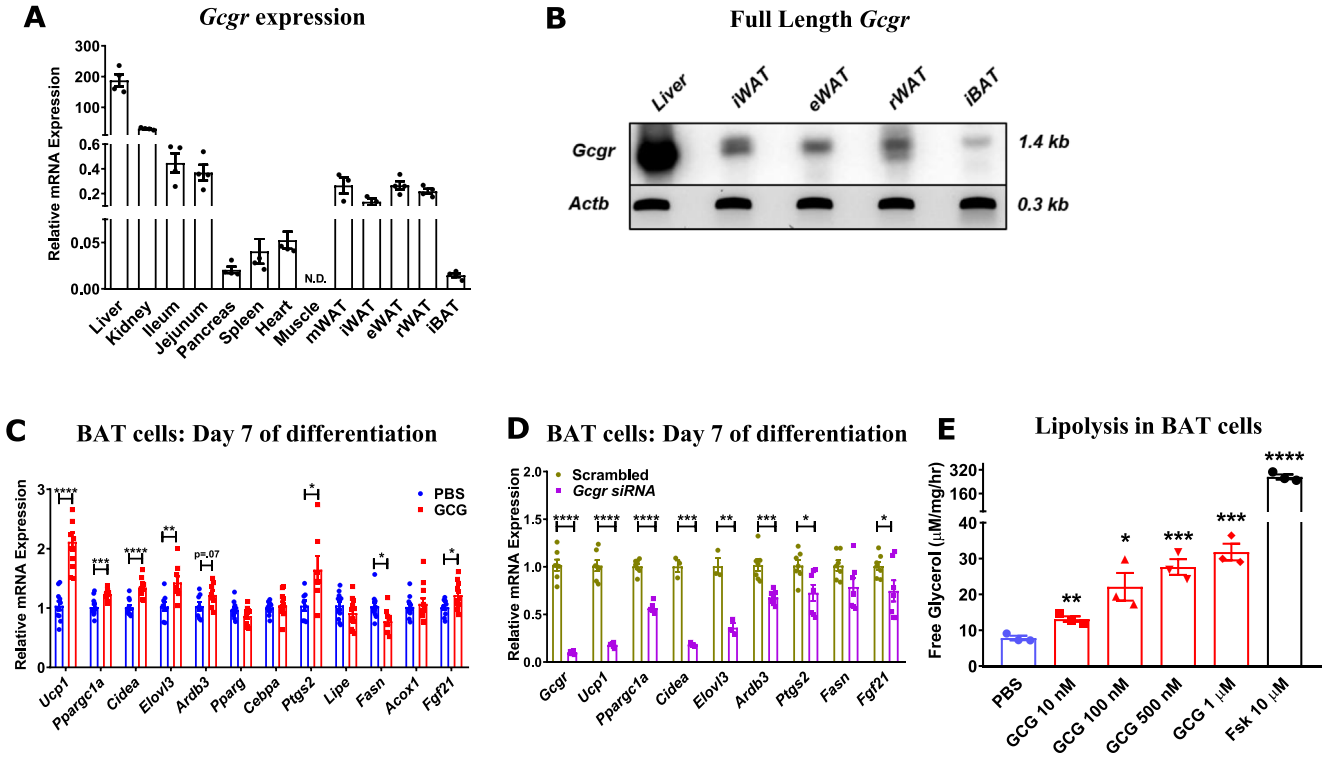

Figure 1: *Gcgr* is expressed in adipose tissue and GCG administration increases thermogenic genes and lipolysis in BAT cells. (A) qPCR analysis of *Gcgr* expression (relative to levels in liver) in tissues from 20 week-old WT mice fed a RCD, n = 4. (B) PCR and Southern blot analysis using *Gcgr*-specific internal oligonucleotide probe detected a full length (~1.4 kb) *Gcgr* mRNA transcript in the liver and adipose tissue; *Actb* PCR of the same samples was used as a control (~0.3 kb). (C) mRNA transcript levels of thermogenic/lipolytic genes in BAT cells (differentiated for 7 days) 1 h after exposure to GCG (100 nM) expressed relative to levels in cells treated with PBS. The data are representative of 3 independent experiments. (D) Basal mRNA transcript levels in differentiated BAT cells transfected with scrambled control or *Gcgr* siRNA. *Tbp* was used as a housekeeping gene for relative mRNA expression levels. (E) Free glycerol release from differentiated BAT cells in response to a 2 h exposure of increasing doses of GCG or forskolin (Fsk, positive control). mWAT = mesenteric white adipose, iWAT = inguinal WAT, eWAT = epididymal WAT, rWAT = retroperitoneal WAT, iBAT = interscapular brown adipose tissue, N.D. = not detectable. *p < 0.05, **p < 0.01, ***p < 0.001, ****p < 0.0001.

MOLECULAR METABOLISM

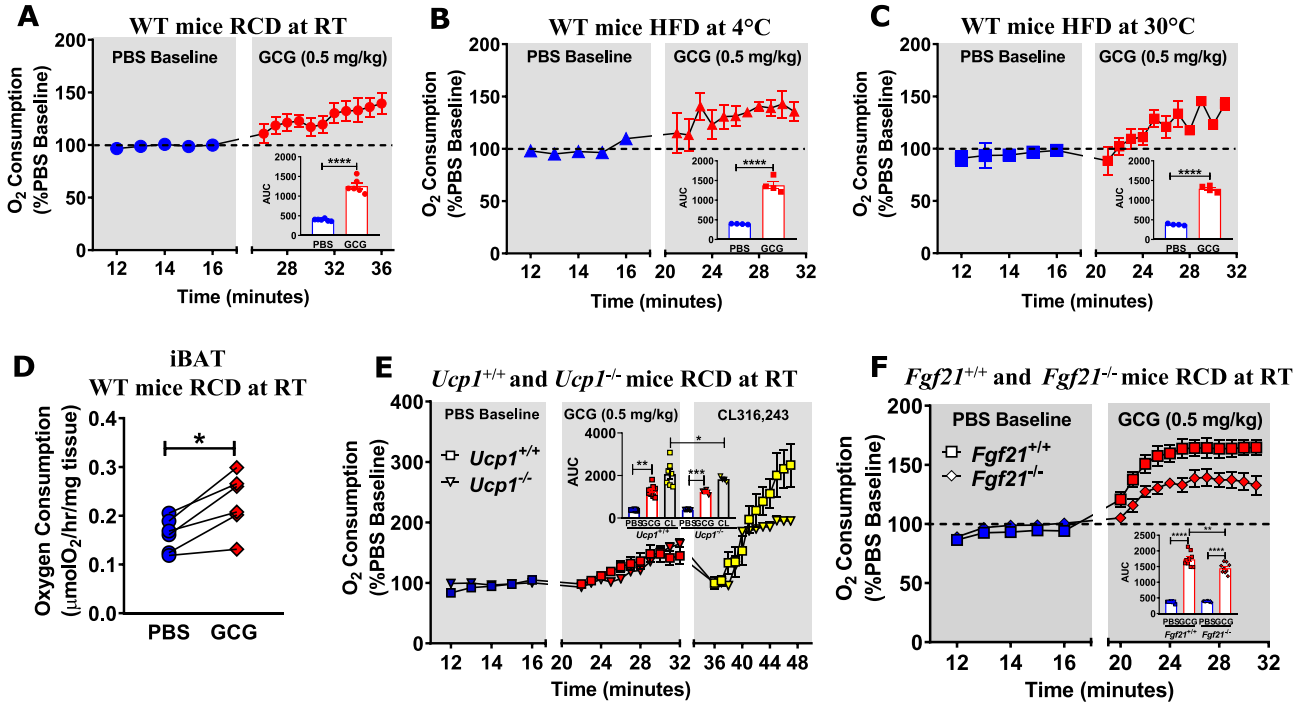

Figure 2: GCG increases oxygen consumption *in vivo* and *ex vivo*, through UCP1-independent and FGF21-dependent pathways. (A) Oxygen consumption following an acute injection of PBS or GCG (0.5 mg/kg) in 8–12 week old WT mice fed a RCD and housed at (A) room temperature (RT, ~21 °C), (B) 4 °C, or (C) 30 °C fed a HFD for 2 weeks, n = 4–6. (D) Oxygen consumption measured in *ex vivo* in iBAT obtained ~ 20–30 minutes after ip administration of PBS or GCG (0.5 mg/kg) to 12 week old WT mice fed a RCD and housed at RT, n = 6. (E) Oxygen consumption in response to an acute injection of PBS, GCG (0.5 mg/kg), or CL316,243, a selective β-3-adrenergic receptor agonist (1.0 mg/kg), 8–12 week old $Ucp1^{+/+}$ and $Ucp1^{-/-}$ mice fed a RCD and housed at RT, n = 6–10. (F) Oxygen consumption following an acute administration of PBS or GCG (0.5 mg/kg) in 12–14 week-old $Fgf21^{+/+}$ and $Fgf21^{-/-}$ mice fed a RCD and housed at RT, n = 10–11. *p < 0.05, **p < 0.01, ***p < 0.001, ****p < 0.0001. iBAT = interscapular brown adipose tissue.

2 weeks while fed a HFD. Acute GCG administration to mice also increased oxygen consumption *ex vivo* in both iBAT and liver explants (Figure 2D and Figure S2D, respectively). GCG increased oxygen consumption to similar levels in $Ucp1^{+/+}$ vs. $Ucp1^{-/-}$ mice, whereas the response to the β-3-adrenergic receptor agonist (CL316,243) was blunted in $Ucp1^{-/-}$ mice (Figure 2E). As circulating FGF21 levels rose rapidly following GCG administration (Figure S2E), we assessed the effect of GCG administration in *Fgf21* null mice. In contrast to observations in *Ucp1* null mice, the GCG-induced rise in oxygen consumption was blunted in $Fgf21^{-/-}$ mice compared to $Fgf21^{+/+}$ control mice (Figure 2F), consistent with recent findings [32].

3.3. Genetic reduction of iBAT *Gcgr* expression does not regulate body weight and composition

To determine whether the BAT *Gcgr* contributes to the physiological control of energy homeostasis or the acute response to GCG agonism, we crossed $Gcgr^{flox/flox}$ with *Myf5*-Cre mice to generate $Gcgr^{BAT-/-}$ mice (Figure 3A). Consistent with the expression domain of *Myf5*, levels of *Gcgr* mRNA transcripts were lower in rWAT and in BAT from $Gcgr^{BAT-/-}$ mice, whereas *Gcgr* expression was not affected in liver, kidney, and jejunum (Figure 3B, Figure S3A). No differences in body weight (Figure 3C), fat and lean mass (Figure 3D), adipose tissue or organ weights (Figure 3E, Figure S3B), or adipose tissue histology (Figure 3F) were detected in RCD-fed or in HFD-fed mice (Figure 3G–J, Figure S3C) housed at RT for 32 weeks. Body temperatures were not different in RCD-fed 8 or 30 week old $Gcgr^{BAT+/+}$ vs. $Gcgr^{BAT-/-}$ mice after a 16 h overnight fast or after 30 weeks on RCD or HFD (Figure S3D and S3E). Basal oxygen consumption was not different in iBAT explants from $Gcgr^{BAT+/+}$ and $Gcgr^{BAT-/-}$ mice after 32 weeks on a RCD (Figure S3F). Hence, the iBAT *Gcgr* is dispensable for control of body weight in response to RCD or HFD-feeding.

3.4. Loss of the iBAT Gcgr does not impact food intake, energy expenditure, or glucose homeostasis

Food intake, energy expenditure, and the respiratory exchange ratio (RER) were not different in older $Gcgr^{BAT+/+}$ vs. $Gcgr^{BAT-/-}$ mice maintained on RCD (Figure 4A–C) or HFD (Figure 4F–H). Moreover, acute administration of GCG to $Gcgr^{BAT+/+}$ and $Gcgr^{BAT-/-}$ mice fed a RCD did not show any differences in oxygen consumption (Figure 4D). Activity levels were not different (Figure S4A and S4D) and the levels of mRNA transcripts for genes regulating thermogenesis or adipose tissue differentiation were similar in adipose tissue depots from RCD- or HFD-fed $Gcgr^{BAT+/+}$ vs. $Gcgr^{BAT-/-}$ mice (Figure 4E,I, Figure S4B,C and S4E,F). Although small increases in plasma GLP-1 and GCG levels were detected in $Gcgr^{BAT-/-}$ fed a RCD (Figure S5B and S5F), no differences in glucose or insulin tolerance, plasma levels of insulin, GCG, and GIP, or adipose tissue gene expression were detected in young RCD- or HFD-fed $Gcgr^{BAT+/+}$ vs. $Gcgr^{BAT-/-}$ mice (Figure S5A-N). Similarly, oral and intraperitoneal glucose tolerance (Figure 5A,B, I and 5J), insulin and lipid tolerance (Figure 5C,D, K and L), plasma levels of TGs and NEFAs (Figure 5E, F, M and N), iBAT TGs (Figure 5G, O), and the relative levels of mRNA transcripts corresponding to genes important for lipid and glucose homeostasis (Figure 5H, P) were not different in older RCD or HFD-fed $Gcgr^{BAT+/+}$ vs. $Gcgr^{BAT-/-}$ mice maintained on diets for a longer period of time.

Original Article

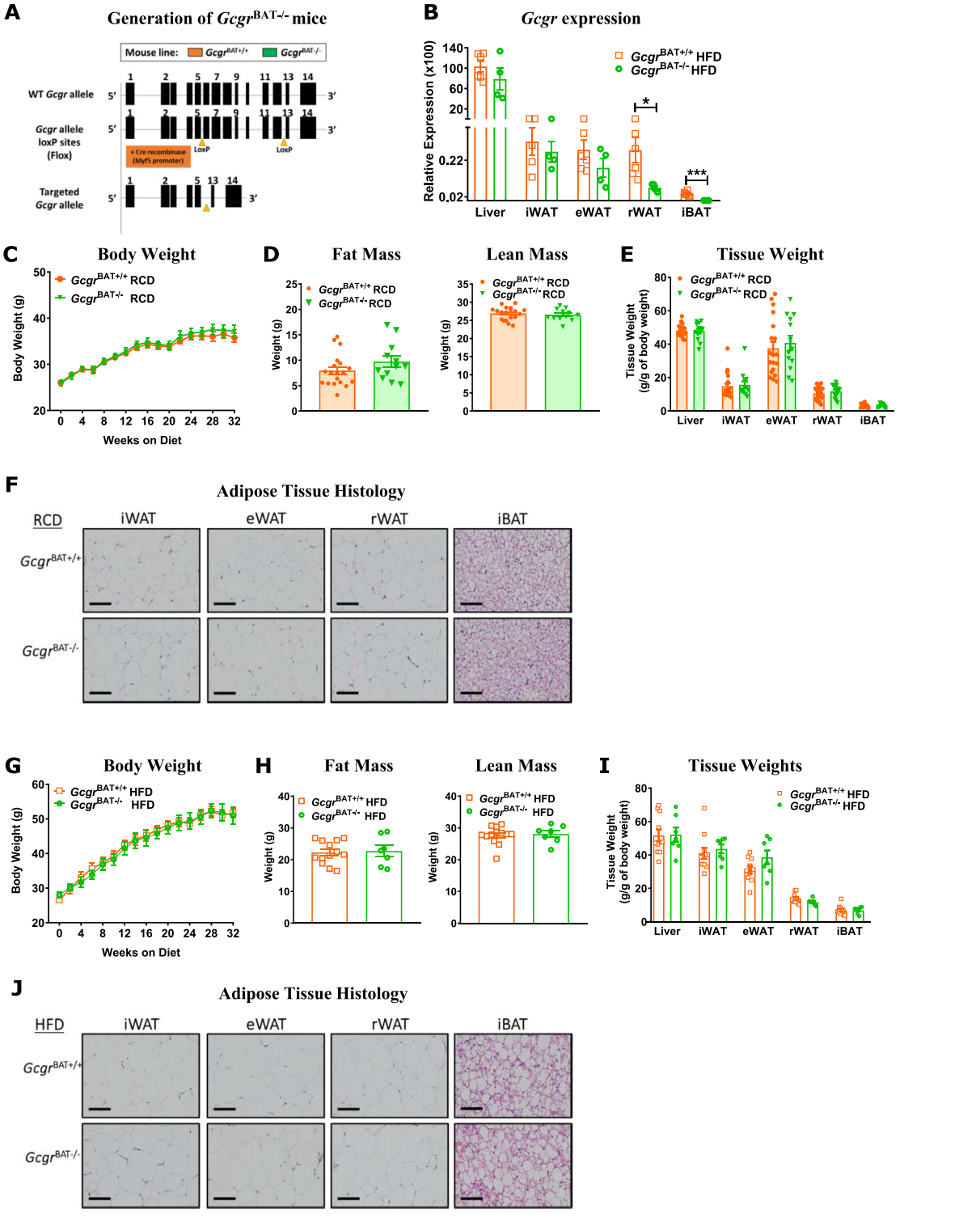

Figure 3: *Gcgr*$^{BAT-/-}$ mice fed RCD or HFD exhibit normal body weight, fat and lean mass, tissue weight, and adipose tissue morphology. (A) Schematic depicting the generation of *Gcgr*$^{BAT-/-}$ mice (B) qPCR analysis of *Gcgr* mRNA expression in liver and adipose tissues from mice fed a HFD for 32 weeks and housed at RT, n = 4–6. (C) Body weights in *Gcgr*$^{BAT+/+}$ and *Gcgr*$^{BAT-/-}$ mice (starting at 8–10 weeks of age) fed a RCD and housed at RT, n = 12–19. Fat and lean mass (D), tissue weights relative to body weight (E), and representative H&E stains of adipose tissue sections, the black bars indicating 100 μM. (F) from *Gcgr*$^{BAT+/+}$ and *Gcgr*$^{BAT-/-}$ mice after 32 weeks of RCD housed at RT, n = 12–19. (G) Body weights of *Gcgr*$^{BAT+/+}$ and *Gcgr*$^{BAT-/-}$ mice (starting at 8–10 weeks of age) fed a HFD and housed at RT, n = 7–14. Fat and lean mass (H), tissue weights relative to body weight (I), and representative H&E stains of adipose tissue sections, the black bars indicate 100 μM (J) from *Gcgr*$^{BAT+/+}$ and *Gcgr*$^{BAT-/-}$ mice after 32 weeks of HFD housed at RT, n = 7–14. *p < 0.05. *Tbp* was used as a housekeeping gene for relative mRNA expression levels. iWAT = inguinal WAT, eWAT = epididymal WAT, rWAT = retroperitoneal WAT, iBAT = interscapular brown adipose tissue.

MOLECULAR METABOLISM

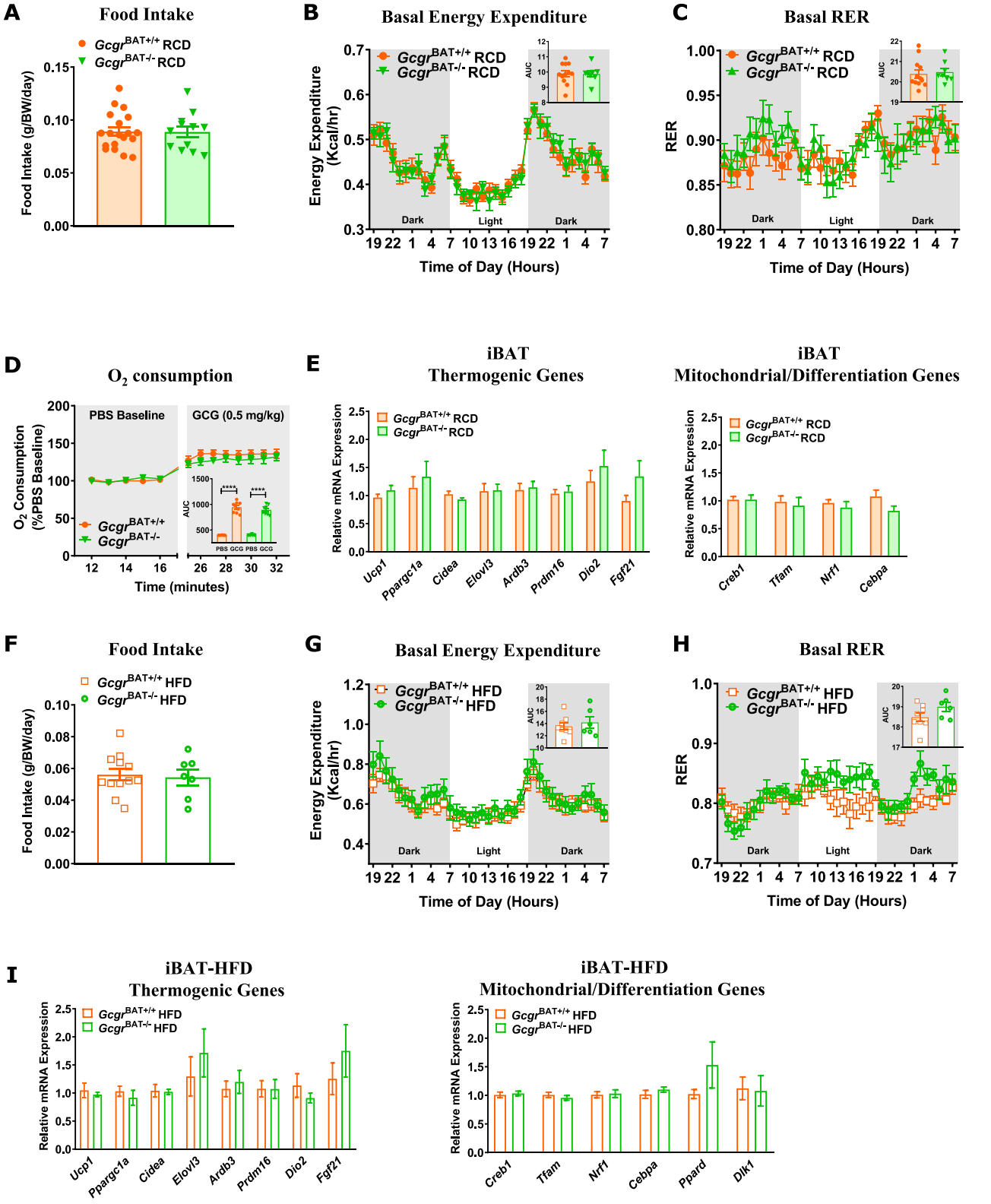

Figure 4: *Gcgr*$^{BAT-/-}$ mice fed a RCD or HFD have normal food intake, energy expenditure, and thermogenic and mitochondrial iBAT mRNA expression profiles. Food intake (A), basal energy expenditure (B) and RER (C) measured over 36 h in *Gcgr*$^{BAT+/+}$ and *Gcgr*$^{BAT-/-}$ mice housed at RT and fed RCD for 28 weeks (A) or 16 weeks (B, C). n = 8–19. (D) Oxygen consumption following an acute injection of PBS or GCG (0.5 mg/kg) in 8-week old *Gcgr*$^{BAT+/+}$ and *Gcgr*$^{BAT-/-}$ mice fed RCD and housed at rt. n = 8–9. (E) iBAT mRNA transcript levels for genes regulating thermogenic, mitochondrial, and differentiation processes in *Gcgr*$^{BAT+/+}$ and *Gcgr*$^{BAT-/-}$ mice fed RCD for 32 weeks housed at RT, n = 4–6. Food intake (F), basal energy expenditure (G) and RER (H) measured over 36 h in *Gcgr*$^{BAT+/+}$ and *Gcgr*$^{BAT-/-}$ mice housed at rt and fed RCD for 28 weeks (F) or 16 weeks (G, H). n = 6–12. (I) iBAT mRNA transcript levels for genes regulating thermogenic, mitochondrial and differentiation processes in *Gcgr*$^{BAT+/+}$ and *Gcgr*$^{BAT-/-}$ mice fed HFD for 32 weeks and housed at RT, n = 4–6. BW = body weight. *Tbp* was used as a housekeeping gene for relative mRNA expression levels. iBAT = interscapular brown adipose tissue.

Original Article

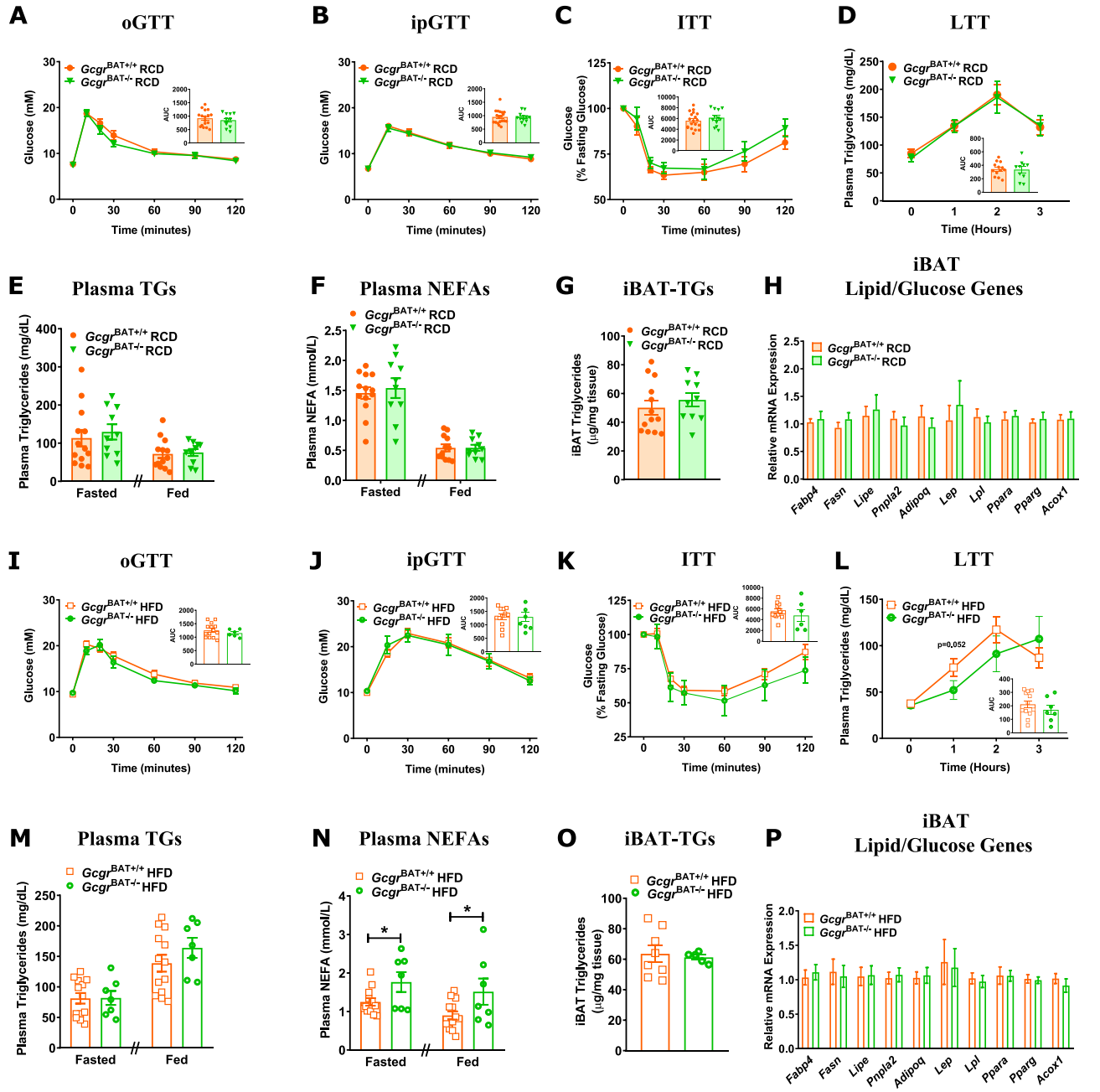

Figure 5: *Gcgr*$^{BAT-/-}$ mice fed RCD or HFD have normal glucose, insulin, and lipid tolerance and glucose and lipid iBAT mRNA expression profiles. Oral glucose tolerance (A, I), ip glucose tolerance (B, J), insulin tolerance (C, K), plasma triglycerides (TGs) measured at 0, 1, 2, and 3 h post oral lipid gavage during a lipid tolerance test (LTT; D, L), plasma TGs (E, M), plasma non-esterified fatty acids (NEFAs) after an overnight fast and 1 h of refeeding (F, N), iBAT TG levels (G, O), and iBAT mRNA transcript levels of lipid and glucose regulatory genes (H, P) in *Gcgr*$^{BAT+/+}$ and *Gcgr*$^{BAT-/-}$ mice housed at RT and fed a RCD (A–H) or HFD (I–P) for 22–32 weeks, n = 10–19 for RCD, n = 7–14 for HFD. *p < 0.05. *Tbp* was used as a housekeeping gene for relative mRNA expression levels. iBAT = interscapular brown adipose tissue.

3.5. Normal metabolic adaptation to cold exposure in *Gcgr*$^{BAT-/-}$ mice

To determine whether the BAT GCGR is important for the metabolic adaptation to chronic cold exposure, we studied HFD-fed *Gcgr*$^{BAT+/+}$ and *Gcgr*$^{BAT-/-}$ mice maintained at 4 °C for ~12 weeks. Body weights (Figure 6A), fat and lean mass and tissue weights (Figure 6B,C), adipose tissue morphology (Figure 6D), food intake, energy expenditure, and respiratory exchange ratio (RER) (Figure 6E–G) were not different between cold-exposed HFD-fed *Gcgr*$^{BAT+/+}$ vs. *Gcgr*$^{BAT-/-}$ mice. Similarly, oral and intraperitoneal glucose tolerance (Figure 6H,I), insulin and lipid tolerance (Figure 6J,K), plasma levels of TGs and NEFAs (Figure 6L, M), iBAT TGs (Figure 6N) and iBAT gene expression profiles (Figure 6O) were also not different between *Gcgr*$^{BAT+/+}$ and *Gcgr*$^{BAT-/-}$ mice exposed to cold and fed a HFD. Furthermore, body temperature (Figure S6A), tissue weights (Figure S6B), basal iBAT oxygen consumption (Figure S6C), and activity levels (Figure S6D) were similar in HFD-fed *Gcgr*$^{BAT+/+}$ and *Gcgr*$^{BAT-/-}$ mice after 10–12 weeks of cold exposure. Collectively, these results demonstrate that BAT GCGR is

MOLECULAR METABOLISM

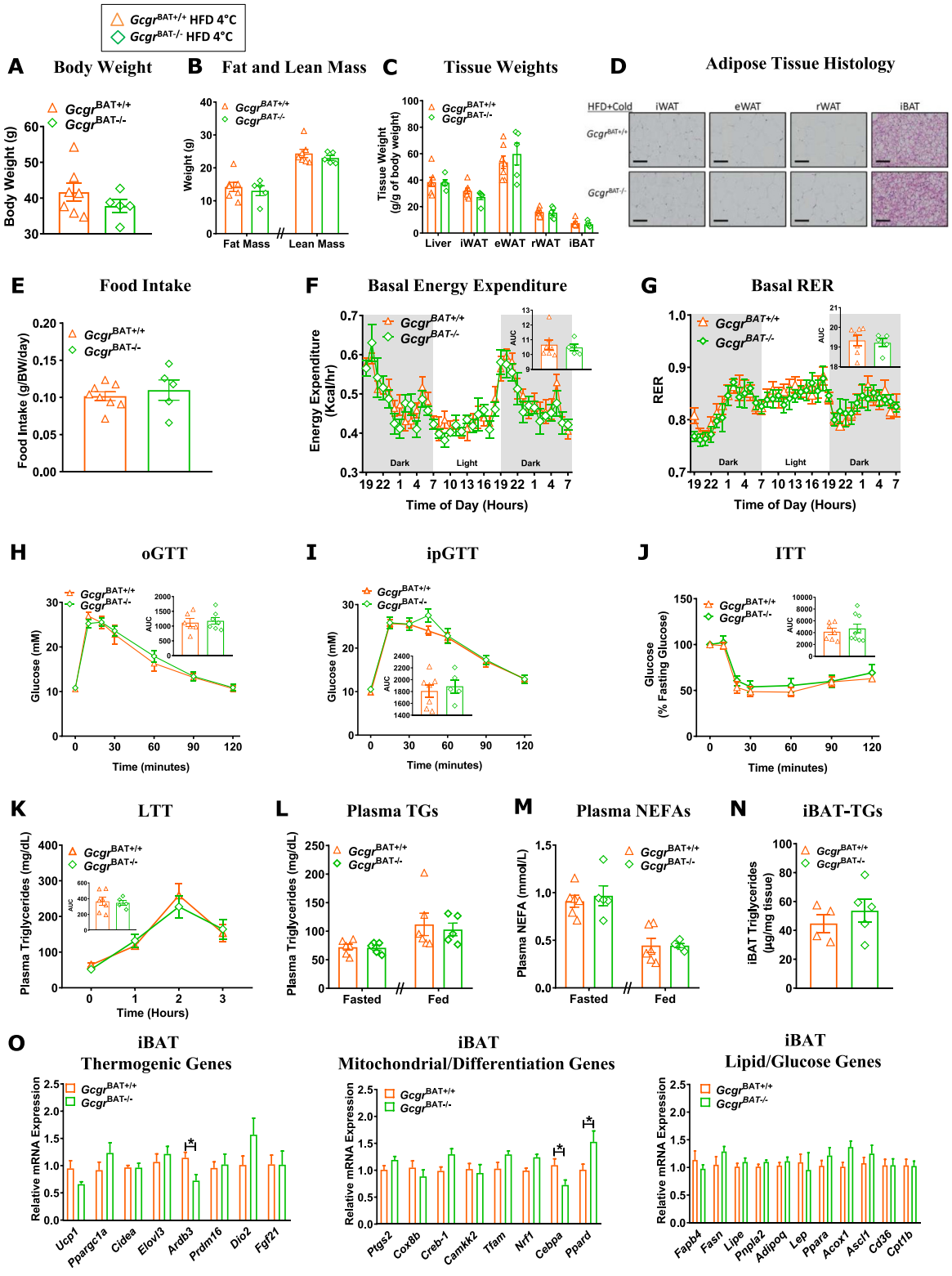

Figure 6: *Gcgr*$^{BAT-/-}$ mice fed a HFD and housed at 4 °C exhibit normal glucose, insulin, and lipid tolerance and energy expenditure. Body weights (A), fat and lean mass (B), tissue weights (C), representative H&E stains of adipose tissue sections, the black bars indicated 100 μM (D), food intake (E), basal energy expenditure measured at RT (F), basal RER (G), oral (H) and ip (I) glucose tolerance, insulin tolerance (J), plasma triglycerides (TGs) measured at 0, 1, 2, and 3 h post oral lipid gavage during a lipid tolerance test (LTT; K), plasma TGs (L), plasma non-esterified fatty acids (NEFAs) after an overnight fast and 1 h of refeeding (M), iBAT TG levels (N), and iBAT mRNA transcript levels of thermogenic, mitochondrial and lipid/glucose regulatory genes, (O) in *Gcgr*$^{BAT+/+}$ and *Gcgr*$^{BAT-/-}$ mice housed at 4 °C and fed a HFD for 2 wks (H), 4 wks (J), 6 wks (I), 8 wks (K), 10 wks (E, F, G), 11 wks (L, M) or 12 wks (A-D, N, O). n = 4–8. *p < 0.05. All mRNA transcript levels were measured relative to levels of the housekeeping gene *Tbp*. iWAT = inguinal WAT, eWAT = epididymal WAT, rWAT = retroperitoneal WAT, iBAT = interscapular brown adipose tissue.

dispensable for the regulation of energy (food intake, energy expenditure, body composition), glucose and lipid metabolism, both in young and old mice, and in mice fed a RCD, or a HFD, and studied at different ambient temperatures.

4. DISCUSSION

Considerable experimentation links acute GCG administration to increased core body temperature [39], BAT blood flow [28], BAT mass, and thermogenic activity [17,23], as well as enhanced energy expenditure in rodents and humans [13,40]. Moreover, several studies have demonstrated direct actions of GCG on BAT [11,41], raising the possibility that GCGR activity contributes to the endogenous control of whole body energy expenditure. Herein, we refine the mechanistic importance of these findings by using mouse genetics to test the relative importance of the murine BAT GCGR for the acute response to GCG administration, and the long term physiological control of energy homeostasis.

Pharmacological GCG agonism produces weight loss through reduction in food intake and via potentiation of thermogenic mechanisms to increase energy expenditure [3,4]. Indeed, GCG-containing peptide multi-agonists require a functional GCGR to reduce fat mass and generate weight loss in HFD-fed mice, actions reflecting a combination of reduced food intake and enhanced energy expenditure [42]. Similarly, the weight loss observed with the GCG-GLP-1 co-agonist MEDI0382 in preclinical studies was partially attributed to GCGR-dependent induction of energy expenditure [43]. Identification of the key tissues essential for the GCGR-dependent control of energy expenditure remains incomplete, and the available evidence supports a role for multiple organs, including liver and adipose tissue, in transducing GCGR-stimulated signals linked to enhanced oxygen consumption [3,32]. Although GCG administration increased *Ucp1* expression in BAT and increased *Fgf2*1 mRNA transcripts in murine liver [12,44], our current data demonstrate that *Ucp1* is not required for acute GCG induction of oxygen consumption.

Consistent with recent independent studies, we confirm that the GCG-induced increase in oxygen consumption is only partially blunted in $Fgf21^{-/-}$ mice [32], implicating additional GCGR-dependent mechanisms contributing to the acute GCG-dependent enhancement of energy expenditure. Notably, glucagon administration may increase oxygen consumption in the liver, adipose tissue, and possibly other tissues [31]. Whether these actions, partially independent of FGF21, reflect additional recruitment of downstream mediators, or direct signaling from the GCGR to mitochondrial pathways, requires further exploration.

Our analysis of relative *Gcgr* gene expression across a range of tissues revealed that levels of adipose tissue *Gcgr* mRNA transcripts were not abundant, being several orders of magnitude lower in WAT compared to liver, and even lower in BAT. Nevertheless, acute administration of GCG to mice increased oxygen consumption not only in the liver, but also in BAT. Furthermore, our studies with BAT cells *in vitro* demonstrated that enhanced or reduced *Gcgr* expression was associated with the regulation of lipolysis and the expression of genes linked to the control of energy expenditure. Hence, to identify a role for the BAT *Gcgr* in the pharmacological response to acute *Gcgr* administration *in vivo*, we generated and characterized $Gcgr^{BAT-/-}$ mice. Unexpectedly, GCG administration robustly induced oxygen consumption to a similar extent in $Gcgr^{BAT+/+}$ vs. $Gcgr^{BAT-/-}$ mice. Taken together, these results suggest that the murine BAT GCGR is not an important molecular target for the acute pharmacological actions of GCG administration, findings consistent with the lack of increased neck temperature or BAT glucose uptake in healthy male humans following transient GCG infusion [15].

The generation of mice with a marked reduction of BAT *Gcgr* expression provided an opportunity to determine the physiological importance of the GCGR within the cellular domains targeted by *Myf5*-Cre. Notably, the BAT *Gcgr* is not required for control of body weight, adiposity, core temperature, or energy expenditure, either when housed at RT or 4 °C. Moreover, we detected no differences in these parameters in mice maintained on a RCD or HFD. Furthermore, glucose homeostasis and lipid tolerance was not different in $Gcgr^{BAT+/+}$ vs. $Gcgr^{BAT-/-}$ mice, whether maintained in the cold, or at RT and studied after exposure to RCD or HFD conditions. Hence, the totality of the data is consistent with the very low level of BAT *Gcgr* expression and reveals that the BAT *Gcgr* is dispensable for metabolic adaptation to energy excess or a cold environment.

5. LIMITATIONS

Our studies have several limitations. First, we focused on acute pharmacological GCG administration in young male C57Bl/6 mice and cannot rule out a role for the BAT GCGR in transduction of a component of weight loss observed with more sustained GCGR agonism in a wider range of mice and conditions [32]. Second, we did not study mice with experimental diabetes; hence, our conclusions are limited to mice analyzed under RCD and HFD feeding. Third, we did not examine the actions of GCG-containing multi-agonists, and it is possible that BAT GCGR activation may be more important when GCG is combined with one or more peptides with complementary metabolic activity. Nevertheless, within the context of these limitations, the results of our studies are quite conclusive and suggest that the BAT GCGR is dispensable for the acute metabolic response to GCG administration and the physiological control of energy homeostasis.

ACKNOWLEDGEMENTS

J.L.B. and E.M.V. have received fellowship funding from Diabetes Canada. E.E.M. has received fellowship funding from the Canadian Diabetes Association and the Canadian Institutes of Health Research. J.E.C. has received fellowships from the Banting and Best Diabetes Centre, University of Toronto, and the Canadian Institutes of Health Research. J.H.S. was supported by the US National Institutes of Health (NIH) grant R00AG055649. P.E.S. was supported by US National Institutes of Health (NIH) grants R01-DK55758, P01-DK088761, R01-DK099110, P01-AG051459 and by an unrestricted grant from the Novo Nordisk Research Foundation.

D.J.D. is supported by Banting and Best Diabetes Centre-Novo Nordisk Chair in Incretin Biology, by Canadian Institutes of Health Research grant 154321 and by operating grant support from Novo Nordisk Inc..

APPENDIX A. SUPPLEMENTARY DATA

Supplementary data to this article can be found online at https://doi.org/10.1016/j.molmet.2019.01.011.

AUTHOR'S CONTRIBUTIONS

Project Design: J.L.B. J.E.C., D.J.D., and P.E.S. Experimental investigation: J.L.B., K.K., E.M.V., L.L.B., X.C., E.E.M., and J.E.C. Formal Analysis: J.L.B., K.K., E.M.V., L.L.B., E.E.M., and J.H.S. Original Written Draft: J.L.B. and D.J.D. Reviewers and Editing: J.L.B., K.K., E.M.V., L.L.B., E.E.M., J.H.S., J.E.C., P.E.S., and D.J.D. Funding Acquisition and Project Administration: D.J.D. Project Supervision: D.J.D. and P.E.S.

CONFLICT OF INTEREST

D.J.D. has served as a speaker for Eli Lilly and as an advisor or consultant to Forkhead Therapeutics, Intarcia, Kallyope, Merck Research Laboratories, Pfizer, Novo

MOLECULAR METABOLISM

Nordisk, and Zafgen. Mt. Sinai receives investigator-initiated funding from Merck, Novo Nordisk, and Shire for preclinical studies of peptide biology in the Drucker laboratory. E.E.M. has received speaker's honoraria from Merck Canada, and the Ottawa Heart Institute receives funding from Merck for preclinical studies in the Mulvihill laboratory. J.E.C. has received speaker honoraria from Merck, and Duke Molecular Physiology Institute receives funding from Eli Lilly for preclinical studies in the Campbell laboratory. The other authors have no other conflicts of interest relevant to this article to disclose.

REFERENCES

[1] Sandoval, D.A., D'Alessio, D.A., 2015. Physiology of proglucagon peptides: role of glucagon and GLP-1 in health and disease. Physiological Reviews 95(2): 513–548.

[2] Habegger, K.M., Heppner, K.M., Geary, N., Bartness, T.J., DiMarchi, R., Tschop, M.H., 2010. The metabolic actions of glucagon revisited. Nature Reviews Endocrinology 6(12):689–697.

[3] Muller, T.D., Finan, B., Clemmensen, C., DiMarchi, R.D., Tschop, M.H., 2017. The new biology and pharmacology of glucagon. Physiological Reviews 97(2): 721–766.

[4] Campbell, J.E., Drucker, D.J., 2015. Islet alpha cells and glucagon–critical regulators of energy homeostasis. Nature Reviews Endocrinology 11(6): 329–338.

[5] Jelinek, L.J., Lok, S., Rosenberg, G.B., Smith, R.A., Grant, F.J., Biggs, S., et al., 1993. Expression cloning and signaling properties of the rat glucagon receptor. Science 259(5101):1614–1616.

[6] Campos, R.V., Lee, Y.C., Drucker, D.J., 1994. Divergent tissue-specific and developmental expression of receptors for glucagon and glucagon-like peptide-1 in the mouse. Endocrinology, 1342156–1342164.

[7] Svoboda, M., Tastenoy, M., Vertongen, P., Robberecht, P., 1994. Relative quantitative analysis of glucagon receptor mRNA in rat tissues. Molecular and Cellular Endocrinology 105(2):131–137.

[8] Hagen, J.H., 1961. Effect of glucagon on the metabolism of adipose tissue. Journal of Biological Chemistry, 2361023–2361027.

[9] Steinberg, D., Vaughan, M., Nestel, P.J., Strand, O., Bergstroem, S., 1964. Effects of the prostaglandins on hormone-induced mobilization of free fatty acids. Journal of Clinical Investigation, 431533–431540.

[10] Richter, W.O., Robl, H., Schwandt, P., 1989. Human glucagon and vasoactive intestinal polypeptide (VIP) stimulate free fatty acid release from human adipose tissue in vitro. Peptides 10(2):333–335.

[11] Joel, C.D., 1966. Stimulation of metabolism of rat brown adipose tissue by addition of lipolytic hormones in vitro. Journal of Biological Chemistry 241(4): 814–821.

[12] Townsend, L.K., Medak, K.D., Knuth, C.M., Peppler, W.T., Charron, M.J., Wright, D.C., 2019. Loss of glucagon signaling alters white adipose tissue browning. The FASEB Journal fj201802048RR.

[13] Davidson, I.W.F., Salter, J.M., Best, C.H., 1960. The effect of glucagon on the metabolic rate of rats. American Journal of Clinical Nutrition 8(5):540–546.

[14] Heim, T., Hull, D., 1966. The effect of propranalol on the calorigenic response in brown adipose tissue of new-born rabbits to catecholamines, glucagon, corticotrophin and cold exposure. Journal of Physiology 187(2):271–283.

[15] Salem, V., Izzi-Engbeaya, C., Coello, C., Thomas, D.B., Chambers, E.S., Comninos, A.N., et al., 2016. Glucagon increases energy expenditure independently of brown adipose tissue activation in humans. Diabetes, Obesity and Metabolism 18(1):72–81.

[16] Schulman, J.L., Carleton, J.L., Whitney, G., Whitehorn, J.C., 1957. Effect of glucagon on food intake and body weight in man. Journal of Applied Physiology 11(3):419–421.

[17] Billington, C.J., Briggs, J.E., Link, J.G., Levine, A.S., 1991. Glucagon in physiological concentrations stimulates brown fat thermogenesis in vivo. American Journal of Physiology Regulatory Integrative and Comparative Physiology 261(2):R501–R507.

[18] Geary, N., Kissileff, H.R., Pi-Sunyer, F.X., Hinton, V., 1992. Individual, but not simultaneous, glucagon and cholecystokinin infusions inhibit feeding in men. American Journal of Physiology 262(6 Pt 2):R975–R980.

[19] Leichter, S.B., 1980. Clinical and metabolic aspects of glucagonoma. Medicine (Baltimore) 59(2):100–113.

[20] Inokuchi, A., Oomura, Y., Nishimura, H., 1984. Effect of intracerebroventricularly infused glucagon on feeding behavior. Physiology & Behavior 33(3):397–400.

[21] Atrens, D.M., Menendez, J.A., 1993. Glucagon and the paraventricular hypothalamus: modulation of energy balance. Brain Research 630(1–2):245–251.

[22] Geary, N., Le Sauter, J., Noh, U., 1993. Glucagon acts in the liver to control spontaneous meal size in rats. American Journal of Physiology 264(1 Pt 2): R116–R122.

[23] Billington, C.J., Bartness, T.J., Briggs, J., Levine, A.S., Morley, J.E., 1987. Glucagon stimulation of brown adipose tissue growth and thermogenesis. American Journal of Physiology 252(1 Pt 2):R160–R165.

[24] Capozzi, M.E., DiMarchi, R.D., Tschop, M.H., Finan, B., Campbell, J.E., 2018. Targeting the incretin/glucagon system with triagonists to treat diabetes. Endocrine Reviews.

[25] Tschop, M.H., Finan, B., Clemmensen, C., Gelfanov, V., Perez-Tilve, D., Muller, T.D., et al., 2016. Unimolecular polypharmacy for treatment of diabetes and obesity. Cell Metabolism 24(1):51–62.

[26] Day, J.W., Ottaway, N., Patterson, J.T., Gelfanov, V., Smiley, D., Gidda, J., et al., 2009. A new glucagon and GLP-1 co-agonist eliminates obesity in rodents. Nature Chemical Biology 5(10):749–757.

[27] Heppner, K.M., Habegger, K.M., Day, J., Pfluger, P.T., Perez-Tilve, D., Ward, B., et al., 2010. Glucagon regulation of energy metabolism. Physiology & Behavior 100(5):545–548.

[28] Yahata, T., Habara, Y., Kuroshima, A., 1983. Effects of glucagon and noradrenaline on the blood flow through brown adipose tissue in temperature-acclimated rats. The Japanese Journal of Physiology 33(3):367–376.

[29] Dicker, A., Zhao, J., Cannon, B., Nedergaard, J., 1998. Apparent thermogenic effect of injected glucagon is not due to a direct effect on brown fat cells. American Journal of Physiology 275(5 Pt 2):R1674–R1682.

[30] Filali-Zegzouti, Y., Abdelmelek, H., Rouanet, J.L., Cottet-Emard, J.M., Pequignot, J.M., Barre, H., 2005. Role of catecholamines in glucagon-induced thermogenesis. Journal of Neural Transmission 112(4):481–489.

[31] Habegger, K.M., Stemmer, K., Cheng, C., Muller, T.D., Heppner, K.M., Ottaway, N., et al., 2013. Fibroblast growth factor 21 mediates specific glucagon actions. Diabetes 62(5):1453–1463.

[32] Kim, T., Nason, S., Holleman, C., Pepin, M., Wilson, L., Berryhill, T.F., et al., 2018. Glucagon receptor signaling regulates energy metabolism via hepatic farnesoid X receptor and fibroblast growth factor 21. Diabetes 67(9):1773–1782.

[33] Kuroshima, A., Yahata, T., 1979. Thermogenic responses of brown adipocytes to noradrenaline and glucagon in heat-acclimated and cold-acclimated rats. The Japanese Journal of Physiology 29(6):683–690.

[34] Svendsen, B., Larsen, O., Gabe, M.B.N., Christiansen, C.B., Rosenkilde, M.M., Drucker, D.J., et al., 2018. Insulin secretion depends on intra-islet glucagon signaling. Cell Reports 25(5):1127–1134 e1122.

[35] Longuet, C., Robledo, A.M., Dean, E.D., Dai, C., Ali, S., McGuinness, I., et al., 2013. Liver-specific disruption of the murine glucagon receptor produces alpha-cell hyperplasia: evidence for a circulating alpha-cell growth factor. Diabetes 62(4):1196–1205.

[36] Panaro, B.L., Coppage, A.L., Beaudry, J.L., Varin, E.M., Kaur, K., Lai, J.H., et al., 2019. Fibroblast activation protein is dispensable for control of glucose homeostasis and body weight in mice. Molecular Metabolism, 1965–1974.

[37] Uldry, M., Yang, W., St-Pierre, J., Lin, J., Seale, P., Spiegelman, B.M., 2006. Complementary action of the PGC-1 coactivators in mitochondrial biogenesis and brown fat differentiation. Cell Metabolism 3(5):333–341.

[38] Arafat, A.M., Kaczmarek, P., Skrzypski, M., Pruszynska-Oszmalek, E., Kolodziejski, P., Szczepankiewicz, D., et al., 2013. Glucagon increases circulating fibroblast growth factor 21 independently of endogenous insulin levels: a novel mechanism of glucagon-stimulated lipolysis? Diabetologia 56(3):588–597.

[39] Doi, K., Kuroshima, A., 1982. Thermogenic response to glucagon in cold-acclimated mice. The Japanese Journal of Physiology 32(3):377–385.

[40] Nair, K.S., 1987. Hyperglucagonemia increases resting metabolic rate in man during insulin deficiency. The Journal of Cinical Endocrinology and Metabolism 64(5):896–901.

[41] Howland, R.J., Bond, K.D., 1987. Modulation by insulin and glucagon of noradrenaline-induced activation of isolated brown adipocytes from the rat. European Journal of Biochemistry 169(1):155–166.

[42] Finan, B., Yang, B., Ottaway, N., Smiley, D.L., Ma, T., Clemmensen, C., et al., 2015. A rationally designed monomeric peptide triagonist corrects obesity and diabetes in rodents. Nature Medicine 21(1):27–36.

[43] Henderson, S.J., Konkar, A., Hornigold, D.C., Trevaskis, J.L., Jackson, R., Fritsch Fredin, M., et al., 2016. Robust anti-obesity and metabolic effects of a dual GLP-1/glucagon receptor peptide agonist in rodents and non-human primates. Diabetes Obesity and Metabolism 18(12):1176–1190.

[44] Kinoshita, K., Ozaki, N., Takagi, Y., Murata, Y., Oshida, Y., Hayashi, Y., 2014. Glucagon is essential for adaptive thermogenesis in brown adipose tissue. Endocrinology 155(9):3484–3492.

Supplementary Table 1. qPCR Primer List

Gene Name	Cat. No.	Manufacturer
Ucp1	Mm01244861_m1	Applied Biosystems
Ppargc1a	Mm00447183_m1	Applied Biosystems
Cidea	Mm00432554_m1	Applied Biosystems
Elovl3	Mm00468164_m1	Applied Biosystems
Ardb3	Mm02601819_g1	Applied Biosystems
Pparg	Mm01184322_m1	Applied Biosystems
Cebpa	Mm00514283_s1	Applied Biosystems
Ptgs2	Mm00478374_m1	Applied Biosystems
Lipe	Mm00495359_m1	Applied Biosystems
Fasn	Mm00662319_m1	Applied Biosystems
Acox1	Mm00443579_m1	Applied Biosystems
Fgf21	Mm00840165_g1	Applied Biosystems
Prdm16	Mm00712556_m1	Applied Biosystems
Dio2	Mm00515664_m1	Applied Biosystems
Fabp4	Mm00445878_m1	Applied Biosystems
Pnpla2	Mm00503040_m1	Applied Biosystems
Adipoq	Mm00456425_m1	Applied Biosystems
Lep	Mm00434759_m1	Applied Biosystems
Lpl	Mm00434764_m1	Applied Biosystems
Nrf1	Mm01135606_m1	Applied Biosystems
Ppard	Mm00803184_m1	Applied Biosystems
Dlk1	Mm00494477_m1	Applied Biosystems
Tfam	Mm00447485_m1	Applied Biosystems
Ppara	Mm00440939_m1	Applied Biosystems
Actb	Mm00607939_s1	Applied Biosystems
Tbp	Mm00446973_m1	Applied Biosystems

Figure S1

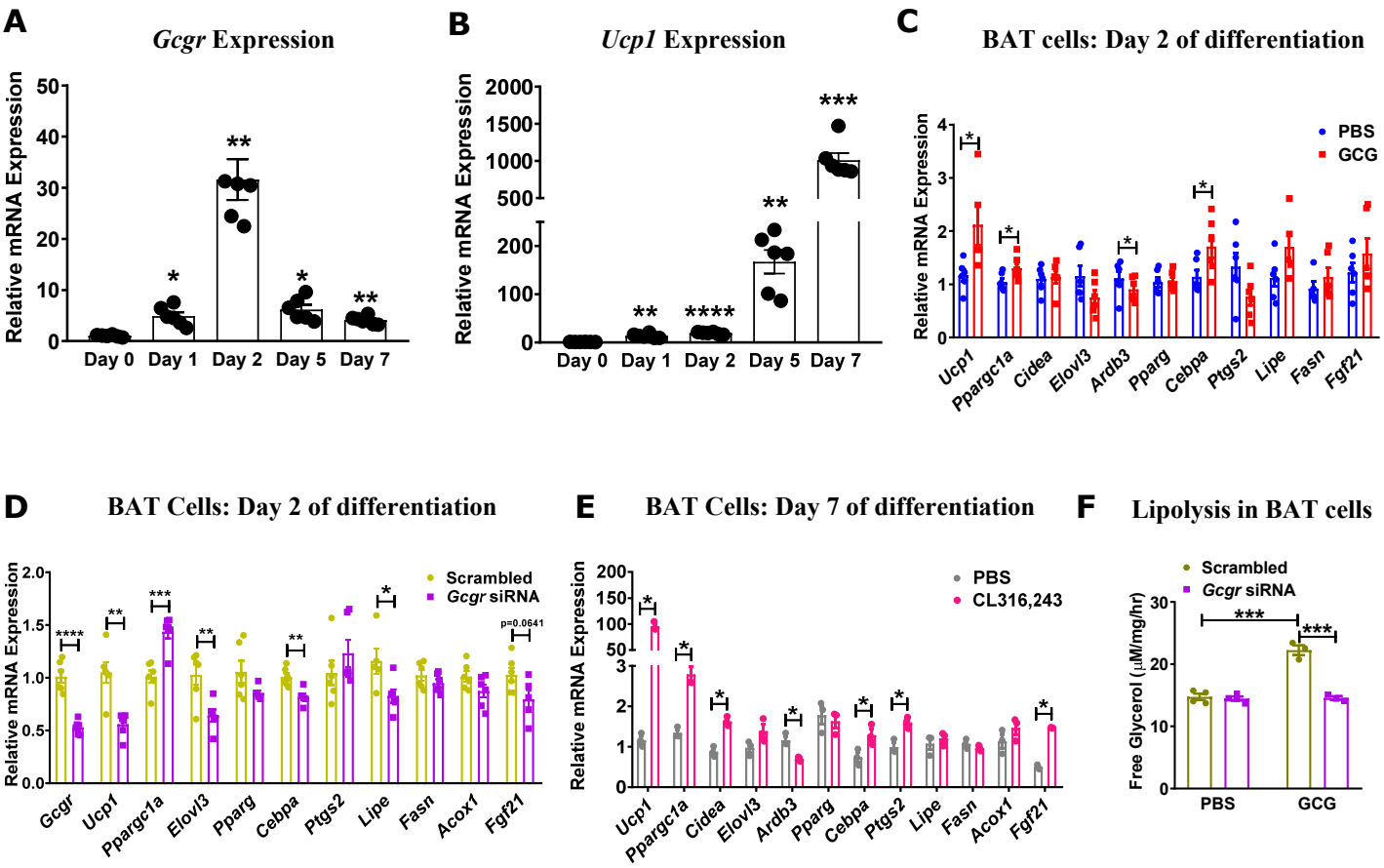
A
Gcgr Expression
Relative mRNA Expression
Day 0
Day 1
Day 2
Day 5
Day 7
B
Ucp1 Expression
Relative mRNA Expression
C
BAT cells: Day 2 of differentiation
Relative mRNA Expression
PBS
GCG
Ucp1
Ppargc1a
Cidea
Elovl3
Ardb3
Pparg
Cebpa
Ptgs2
Lipe
Fasn
Fgf21
D
BAT Cells: Day 2 of differentiation
Relative mRNA Expression
Scrambled
Gcgr siRNA
p=0.0641
Gcgr
Ucp1
Ppargc1a
Elovl3
Pparg
Cebpa
Ptgs2
Lipe
Fasn
Acox1
Fgf21
E
BAT Cells: Day 7 of differentiation
Relative mRNA Expression
PBS
CL316,243
F
Lipolysis in BAT cells
Free Glycerol (μM/mg/hr)
Scrambled
Gcgr siRNA
PBS
GCG

Figure S2

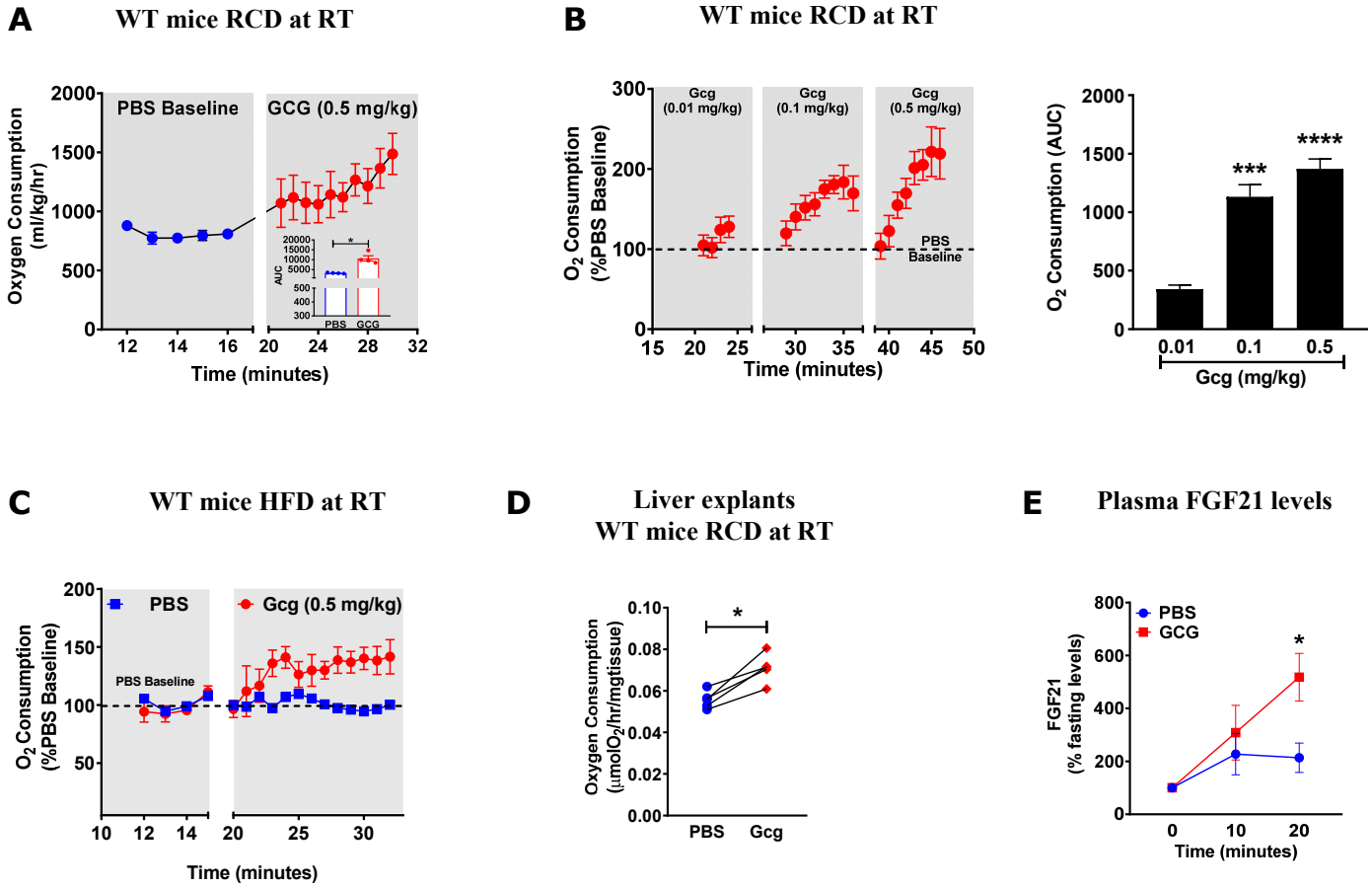
A
WT mice RCD at RT
PBS Baseline
GCG (0.5 mg/kg)
Oxygen Consumption (ml/kg/hr)
Time (minutes)
AUC
PBS
GCG
B
WT mice RCD at RT
Gcg (0.01 mg/kg)
Gcg (0.1 mg/kg)
Gcg (0.5 mg/kg)
PBS Baseline
O2 Consumption (%PBS Baseline)
Time (minutes)
O2 Consumption (AUC)
Gcg (mg/kg)
C
WT mice HFD at RT
PBS
Gcg (0.5 mg/kg)
PBS Baseline
O2 Consumption (%PBS Baseline)
Time (minutes)
D
Liver explants
WT mice RCD at RT
Oxygen Consumption (µmolO2/hr/mgtissue)
PBS
Gcg
E
Plasma FGF21 levels
PBS
GCG
FGF21 (% fasting levels)
Time (minutes)

Figure S3

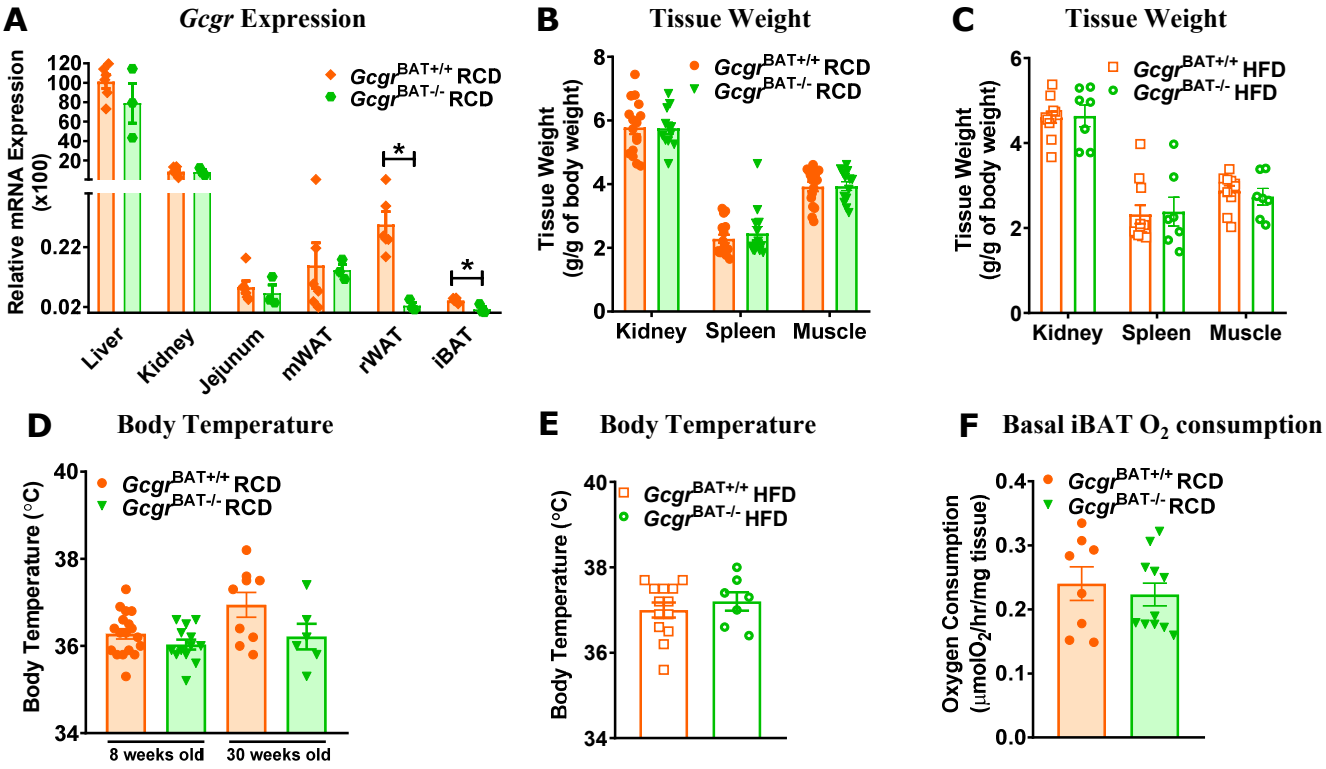
A
Gcgr Expression
Relative mRNA Expression (x100)
Gcgr BAT+/+ RCD
Gcgr BAT-/- RCD
Liver
Kidney
Jejunum
mWAT
rWAT
iBAT
B
Tissue Weight
Tissue Weight (g/g of body weight)
Kidney
Spleen
Muscle
C
Tissue Weight
Gcgr BAT+/+ HFD
Gcgr BAT-/- HFD
D
Body Temperature
Body Temperature (°C)
8 weeks old
30 weeks old
E
Body Temperature
F
Basal iBAT O2 consumption
Oxygen Consumption (μmolO2/hr/mg tissue)

Figure S4

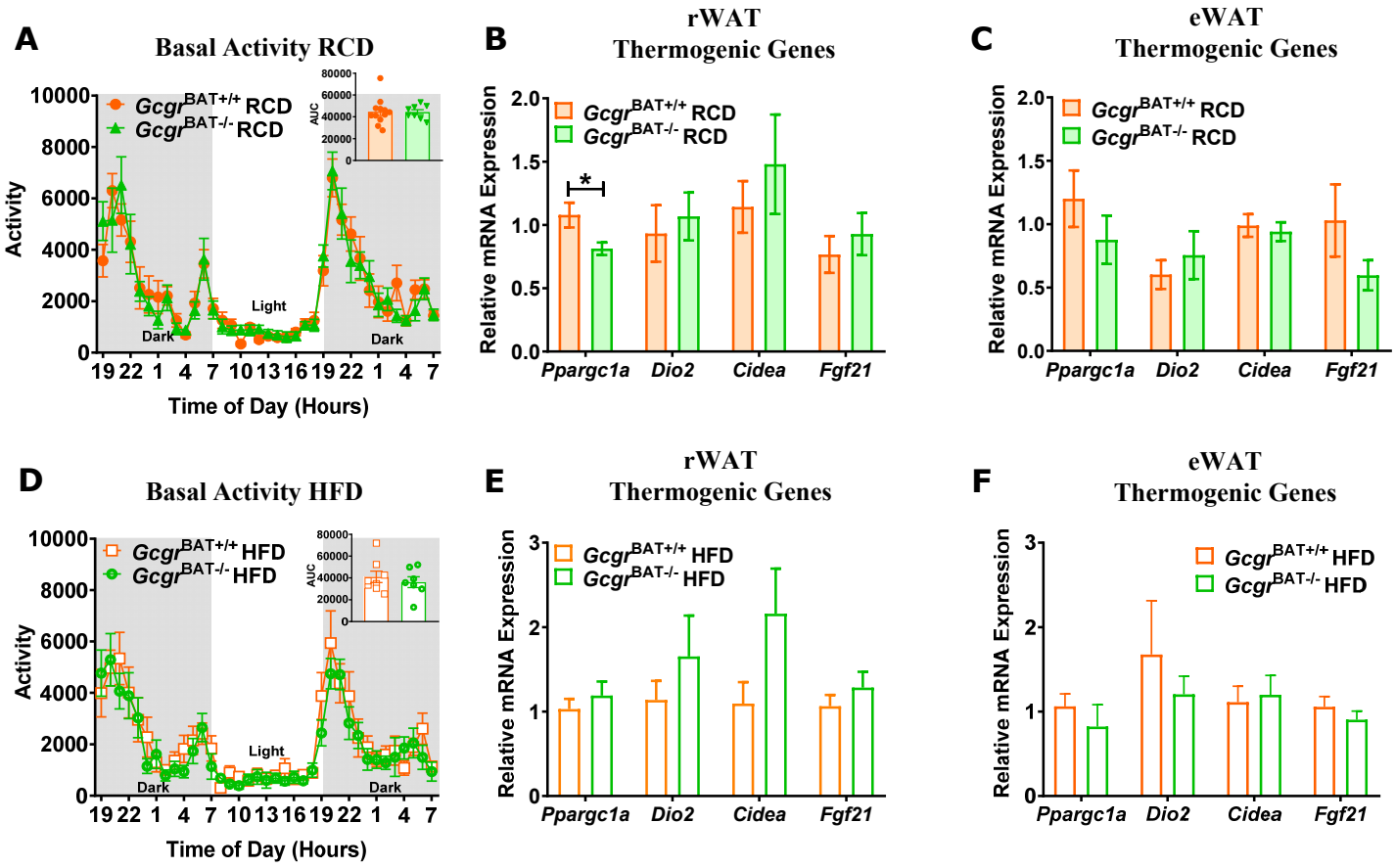
A
Basal Activity RCD
Gcgr BAT+/+ RCD
Gcgr BAT-/- RCD
Activity
Light
Dark
Dark
Time of Day (Hours)
AUC
B
rWAT
Thermogenic Genes
Relative mRNA Expression
*
Ppargc1a
Dio2
Cidea
Fgf21
C
eWAT
Thermogenic Genes
D
Basal Activity HFD
E
rWAT
Thermogenic Genes
F
eWAT
Thermogenic Genes

Figure S5

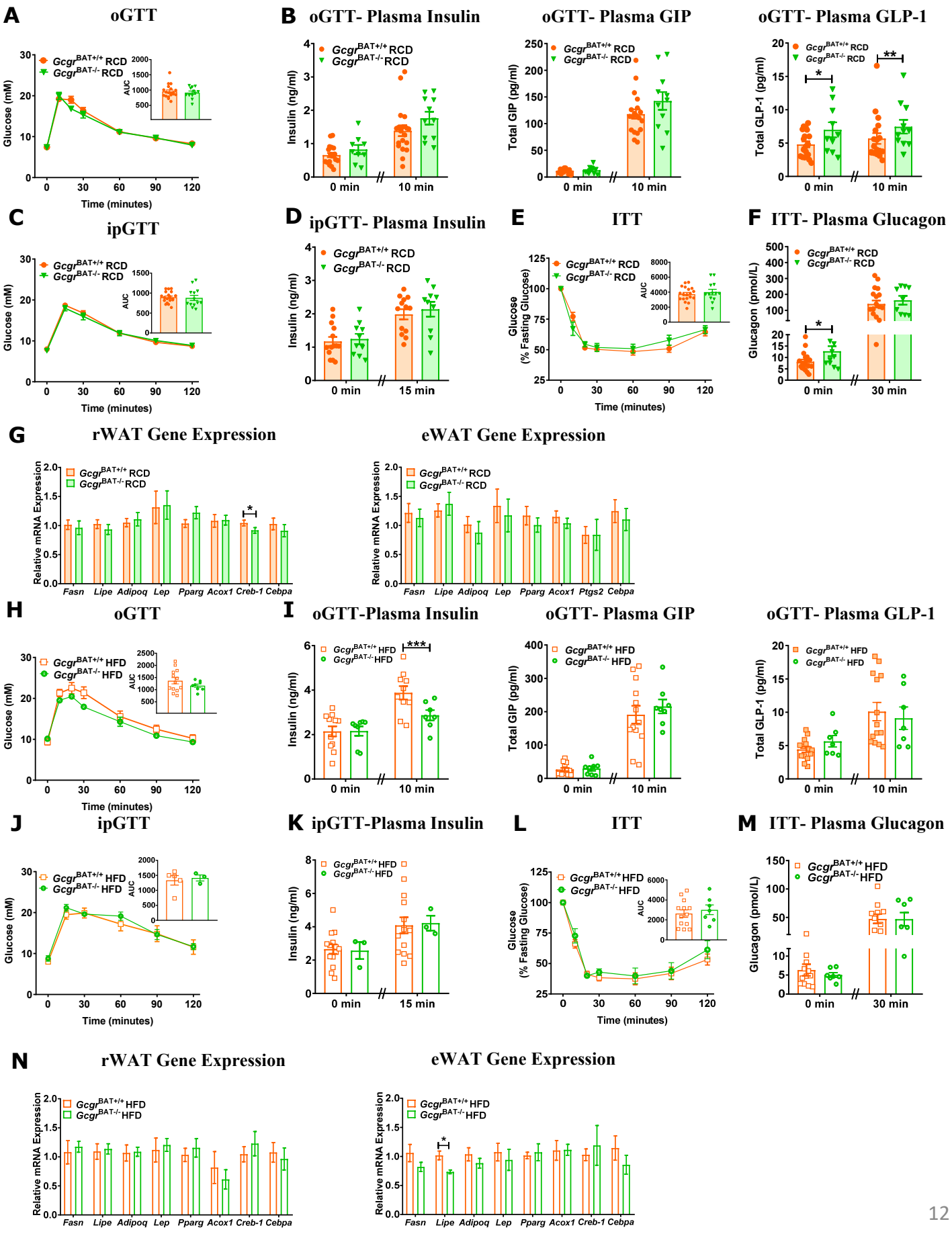
A
oGTT
Glucose (mM)
Time (minutes)
AUC
B
oGTT- Plasma Insulin
Insulin (ng/ml)
oGTT- Plasma GIP
Total GIP (pg/ml)
oGTT- Plasma GLP-1
Total GLP-1 (pg/ml)
0 min
10 min
C
ipGTT
D
ipGTT- Plasma Insulin
15 min
E
ITT
Glucose (% Fasting Glucose)
F
ITT- Plasma Glucagon
Glucagon (pmol/L)
30 min
G
rWAT Gene Expression
eWAT Gene Expression
Relative mRNA Expression
Fasn Lipe Adipoq Lep Pparg Acox1 Creb-1 Cebpa
Ptgs2
H
oGTT
I
oGTT-Plasma Insulin
J
ipGTT
K
ipGTT-Plasma Insulin
L
ITT
M
ITT- Plasma Glucagon
N
rWAT Gene Expression
eWAT Gene Expression
RCD
HFD

Figure S6

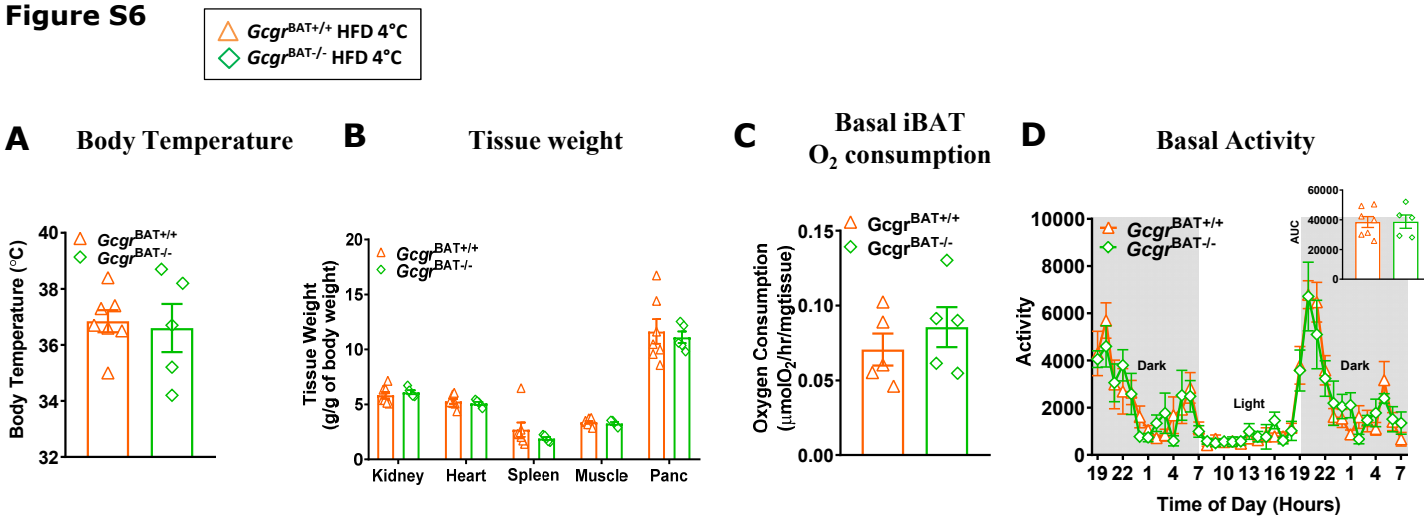
GcgrBAT+/+ HFD 4°C
GcgrBAT-/- HFD 4°C
A
Body Temperature
Body Temperature (°C)
B
Tissue weight
Tissue Weight (g/g of body weight)
Kidney
Heart
Spleen
Muscle
Panc
C
Basal iBAT O2 consumption
Oxygen Consumption (µmolO2/hr/mgtissue)
D
Basal Activity
Activity
Dark
Light
Dark
Time of Day (Hours)
AUC